arXiv:cond-mat/0202240v2 [cond-mat.mtrl-sci] 5 Jul 2002

Stability and electronic structure in hexagonal $\beta\,\mathrm{Al_9Mn_3Si}$ and $\varphi\,\mathrm{Al_{10}Mn_3}$ crystals

Guy Trambly de Laissardière

Laboratoire de Physique Théorique et Modélisation, CNRS–Université de
Cergy-Pontoise (ESA 8089), 5 mail Gay-Lussac, Neuville sur Oise, 95031
Cergy-Pontoise, France

E-mail: `guy.trambly@ptm.u-cergy.fr`

Abstract. The electronic structures of hexagonal $\beta\,\mathrm{Al_9Mn_3Si}$ and $\varphi\,\mathrm{Al_{10}Mn_3}$ are investigated through self-consistent calculations carried out using the LMTO method. This *ab initio* approach is combined with an analysis of a simplified hamiltonian model for Al based alloys containing transition metal atoms. Results show a strong effect on an atomic structure stabilisation by an indirect Mn-Mn interaction mediated by conduction electrons over medium range distances (5 Å and more). Both the role and position of Si atoms are explained as well as the origin of large vacancies which characterises these atomic structures. As β and φ phases are related to Al based quasicrystals and related approximant structures, it yields arguments on the stabilisation of such complex phases.

PACS numbers:
61.50.Lt, Crystal binding; cohesive energy
61.44.Br, Quasicrystals
71.20.Lp, Intermetallic compounds
71.23.Ft, Quasicrystals

Submitted to: *J. Phys.: Condens. Matter*

2002/7/5

1. Introduction

The almost isomorphic stable $\beta\,\mathrm{Al_9Mn_3Si}$ [1] and metastable $\varphi\,\mathrm{Al_{10}Mn_3}$ [2] phases are often present in alloys containing quasicrystals in Al(Si)-Mn systems. Although their diffraction features are different from those of quasicrystals, several correlations with quasiperiodic atomic structure have been shown. For instance, there is a strong resemblance of these phases with parts of the complex structures of $\mu\,\mathrm{Al_{4.12}Mn}$ [3] and $\lambda\,\mathrm{Al_4Mn}$ [4] which are related to quasicrystals. β and φ are also almost isomorphic with $\mathrm{Al_5Co_2}$ [5] which is an approximant of decagonal quasicrystal with the shortest periodic stacking sequence along the tenfold axis [6].

Meta-stable icosahedral (*i*-) and decagonal (*d*-) quasicrystals have been found in the Al-Mn system [7, 8, 9]. With the addition of few per cent of Si atoms, new stable phases are obtained: *i*-Al-Mn-Si [8], approximant $\alpha\,\mathrm{Al_9Mn_2Si}$ [10, 11, 12] and $\beta\,\mathrm{Al_9Mn_3Si}$... The occurrence of stable complex structure in Al-Mn and Al-Mn-Si is a major question in the understanding of the stability of quasicrystals. For instance, the role of Si in stabilising the *i*-phase, is not yet understood. In this direction, investigations on relations between isomorphic stable $\beta\,\mathrm{Al_9Mn_3Si}$ and meta-stable $\varphi\,\mathrm{Al_{10}Mn_3}$ phases represent a great interest. On another hand, these phases give a good example to analyse the effect of the position of transition metal (TM) atoms in stabilising complex structure related to quasiperiodicity.

In this paper, a first-principles (*ab initio*) study of the electronic structure in $\beta\,\mathrm{Al_9Mn_3Si}$ and $\varphi\,\mathrm{Al_{10}Mn_3}$ phases is combined with a model approach in order to describe the interplay between the medium range order and the electronic structure. Results are compared between β, φ, $\mathrm{Al_5Co_2}$, $\mu\,\mathrm{Al_{4.12}Mn}$, and $\lambda\,\mathrm{Al_4Mn}$ phases. The stabilising role of Si and the origin of a large hole (vacancy) in both β and φ phases are justified. The origin of a pseudogap is analysed in the frame of the Hume-Rothery stabilisation rule for sp-d electron phases [13, 14]. Besides, a real space approach in term of a realistic TM-TM pair interaction allows to understand the effect of Mn position. As these phases are related to quasiperiodic phases, such a study yields arguments to discuss the interplay between electronic structure and stability in quasicrystals.

The paper is organised as follows. In section 2, is presented a short review on Hume-Rothery mechanism in Al(rich)-TM phases that has often been proposed for the stabilisation of crystals and quasicrystals. The structures of φ and β are presented in section 3 with a discussion on their relations with quasicrystals. First-principles (*ab initio*) study of the electronic structure is presented in section 4. Then the effect of the sp-d hybridisation is analysed in details through *ab initio* calculations for hypothetical structures. In section 5, these results are understood in term of a Friedel-Anderson sp-d hamiltonian that allows to find the *"effective Bragg potential"* for sp-d Hume-Rothery alloys. In section 6, a real space approach of the Hume-Rothery mechanism shows the strong effect of a medium range Mn-Mn pair interaction (up to $\sim 5\,\text{Å}$ and more). Magnetism is studied in section 7 and a short conclusion is given in section 8.

2. Hume-Rothery stabilisation in quasicrystals and related crystals

2.1. Near contact between Fermi sphere and pseudo-Brillouin zone

Since the 1950s, Al(rich)-TM crystals are considered by many authors as Hume-Rothery alloys [15] (for instance see Refs [16, 17, 18, 19, 20, 1, 2]). In these phases, the important parameter is the average number of electrons per atom, e/a. The valence of Al and Si are fixed without ambiguity (+3 and +4, respectively). Following classical theory [19, 20], a negative valence is assigned to TM atom (typically, -3 for Mn, -2 for Fe, -1 for Co and 0 for Ni). For $\varphi\,Al_{10}Mn_3$, $\beta\,Al_9Mn_3Si$ and Al_5Co_2, e/a is equal to 1.61, 1.69 and 1.86, respectively. The occurrence of different compounds with similar structures is therefore to be explained by the fact that they are electron compounds with similar e/a ratio in spite of different atomic concentrations [1]. Indeed, for these phases a band energy minimisation occurs when the Fermi sphere touches a pseudo-Brillouin zone (prominent Brillouin zone), constructed by Bragg vectors $\mathbf{K}_p$ corresponding to intense peaks in the experimental diffraction pattern. The Hume-Rothery condition for alloying is then $2k_F \simeq K_p$. Assuming a free electron valence band, the Fermi momentum, k_F, is calculated from e/a.

Soon after the discovery of quasicrystals, it has been pointed out that their stoechiometry appears to be governed by a Hume-Rothery rule (see for instance [21, 22, 23, 24, 25, 26, 27, 28]). Indeed the e/a ratio has been used for a long time to distinguish between Frank-Kasper type quasicrystals (sp quasicrystals) and Mackay type quasicrystals (sp-d quasicrystals) [25]. Friedel and Dénoyer [21] have determined the pseudo-Brillouin zone in contact with the Fermi sphere for *i*-Al-Li-Cu. Gratias et al. [29] have shown that the Al-Cu-Fe icosahedral domain is located along a line in the phase diagram defined by the equation e/a $\simeq$ 1.86. Besides, Al-Cu-Fe alloys along an e/a-constant line have similar local electronic properties and local atomic order [30]. Recently, a pseudo-Brillouin zone that touches the Fermi Sphere in 1/1 Al-Cu-Ru-Si and Al-Mg-Zn approximants has been identified [31, 32]. With the discovery of decagonal *d*-Al-Cu-Co and *d*-Al-Ni-Co by Tsai et al. [33], these authors [25] have determined that the value of e/a ratio is about 1.7 in spite of wide composition range for quasicrystals in these systems. The importance of e/a value in quasicrystals and their properties suggests that Hume-Rothery mechanism plays a significant role in their stabilisation.

2.2. Pseudogap in the density of states

The density of states (DOS) in sp Hume-Rothery alloys is well described by the *Jones theory* (for review see Refs [34, 35, 36]). The valence band (sp states) are nearly-free electrons, and the Fermi-sphere / pseudo-Brillouin zone interaction creates a depletion in the DOS, called "*pseudogap*", near the Fermi energy, E_F. This pseudogap has been found both experimentally and from first-principles calculations in classical Hume-Rothery alloys (see for instance the recent theoretical study of archetypal system Cu-Zn [35]). It has also been found experimentally and theoretically in sp quasicrystals and related phases (for instance in Al-Li-Cu [8, 26] and Al-Mg-Zn [27, 31]). But, the treatment of Al(rich) alloys containing transition metal elements requires a new theory. Indeed, the d states of TM are not nearly-free states in spite of strong sp-d hybridisation. Thus a model for sp-d electron phases which combined the effect of the diffraction by Bragg planes with the sp-d hybridisation has been developped [13, 14]. It is shown that negative valence of TM atom results from particular effects of the sp-d hybridisation in Hume-Rothery alloys [22, 37, 13, 14]. Besides the TM DOS (mainly d states) depends strongly on TM atoms positions. For particular TM positions, one obtains a pseudogap near E_F in total DOS and partial d DOS. This has been confirmed by *ab initio* calculations in a series of Al(rich)-TM crystals including Al_5Co_2 [14],which is isomorphic with $\beta\,Al_9Mn_3Si$ and $\varphi\,Al_{10}Mn_3$. The presence of a pseudogap in Al_5Co_2 DOS has also been confirmed by photoemission spectroscopy [38]. For icosahedral sp-d quasicrystals and their approximants, a wide pseudogap at E_F has been found experimentally [8, 39, 40, 41, 42, 43, 44] and from *ab initio* calculations [24, 45, 46, 47, 32]. For instance in *i*-Al-Cu-Fe, *i*-Al-Pd-Mn and α Al-Mn-Si, the DOS at E_F is reduced by $\sim 1/3$ with respect to pure Al (c.f.c.) DOS [8].

However, there are contradictory results about DOS in decagonal quasicrystals. Photoemission spectroscopy measurements in the photon-energy range 35-120 eV do not show any pseudogap [48] in *d*-$Al_{65}Co_{15}Cu_{20}$ and *d*-$Al_{70}Co_{15}Ni_{15}$, whereas ultrahigh resolution ultraviolet photoemission shows a depletion of the DOS at E_F for the same compositions [49]. From soft X-ray spectroscopy, DOS in *d*-$Al_{65}Co_{20}Cu_{15}$ and *d*-$Al_{70}Co_{15}Ni_{15}$, exhibits also a pseudogap in the Al-3p band [50]. Recently a pseudogap, enhanced by sp-d hybridisation, has been found in the Al-p band of *d*-Al-Pd-Mn [44]. There are also *ab initio* calculations performed for several atomic model approximants of *d*-Al-Cu-Co [51, 52], *d*-Al-Co-Ni [53] and *d*-Al-Pd-Mn [54]. The results show that an existence of pseudogap depends on the position of the TM atoms. Indeed, some TM atoms may "fill up" the pseudogap, via the sp-d hybridisation; whereas other TM positions enhance the pseudogap.

In summary, the importance of Hume-Rothery mechanism is now established for many Al-based quasicrystals with and without TM elements although the presence of a pseudogap near E_F is still discussed for decagonal phases. Nevertheless, one can not ignore the possible Hume-Rothery stabilising effect on the origin of the quasiperiodicity. This is the reason why in this article *ab initio* results are analysed in the frame work of Hume-Rothery mechanism in order to test the importance of this mechanism.

3. Structures and relations with quasicrystals

3.1. General aspects

The unit cell dimensions of $\beta\,Al_9Mn_3Si$ [1] and $\varphi\,Al_{10}Mn_3$ [2] are similar, with a same space group $P6_3/mmc$. Atomic environment and interatomic distances are gathered in tables 1 and 2.

Table 1. Lattice parameters and atomic positions of hexagonal $\beta\,\mathrm{Al_9Mn_3Si}$, $\varphi\,\mathrm{Al_{10}Mn_3}$ and $\mathrm{Al_5Co_2}$ phases of $\mathrm{P6_3/mmc}$ space group.

Lattice parameters	$\beta\,\mathrm{Al_9Mn_3Si}$ [1]		$\varphi\,\mathrm{Al_{10}Mn_3}$ [2]		$\mathrm{Al_5Co_2}$ [5]	
a (Å)	7.513		7.543		7.656	
c (Å)	7.745		7.898		7.593	
Wyckoff Sites						
(2a) : 0, 0, 0	(Al,Si)(0)		Al(0)		Al(0)	
(6h) : x,$2x$,$\frac{1}{4}$	(Al,Si)(1)	$x = .4579$	Al(1)	$x = .4550$	Al(1)	$x = .4702$
(12k) : x,$2x$,z	(Al,Si)(2)	$x = .2006$	Al(2)	$x = .1995$	Al(2)	$x = .1946$
		$z = -.0682$		$z = -.0630$		$z = -.0580$
(6h) : x,$2x$,$\frac{1}{4}$	Mn	$x = .1192$	Mn	$x = .1215$	Co(1)	$x = .1268$
(2d) : $\frac{2}{3}$,$\frac{1}{3}$,$\frac{1}{4}$	Va		Va		Co(0)	

Table 2. Interatomic distances in $\beta\,\mathrm{Al_9Mn_3Si}$, $\varphi\,\mathrm{Al_{10}Mn_3}$ and $\mathrm{Al_5Co_2}$. TM is either Mn or Co(1). X corresponds to the vacancy in β and φ phases and to Co(0) in $\mathrm{Al_5Co_2}$.

Atom	Wyckoff site	Neighbours	Distances (Å) $\beta\,\mathrm{Al_9Mn_3Si}$	$\varphi\,\mathrm{Al_{10}Mn_3}$	$\mathrm{Al_5Co_2}$
Al,Si(0)	(2a)	6 Al(2)	2.66	2.65	2.62
		6 TM(1)	2.48	2.53	2.53
Al(1)	(6h)	2 Al(1)	2.81	2.75	3.14
		4 Al(2)	2.77	2.84	2.74
		4 Al(2)	2.98	2.99	2.97
		2 TM(1)	2.42	2.41	2.41
		1 X	2.72	2.77	2.61
Al(2)	(12k)	1 Al,Si(0)	2.66	2.65	2.62
		2 Al(1)	2.77	2.84	2.74
		2 Al(1)	2.98	2.99	2.97
		2 Al(2)	2.81	2.79	2.73
		1 Al(2)	2.82	2.95	2.92
		2 Al(2)	2.99	3.03	3.19
		1 TM(1)	2.68	2.67	2.51
		2 TM(1)	2.68	2.71	2.70
		1 X	2.23	2.29	2.35
TM(1)	(6h)	2 Al,Si(0)	2.48	2.53	2.54
		2 Al(1)	2.42	2.41	2.41
		2 Al(2)	2.68	2.67	2.51
		4 Al(2)	2.68	2.71	2.70
		2 TM(1)	2.69	2.75	2.91
X	(2d)	3 Al(1)	2.72	2.77	2.61
		6 Al(2)	2.23	2.29	2.35
		6 TM(1)*	3.81	3.82	3.86

* X and TM(1) are not first-neighbour.

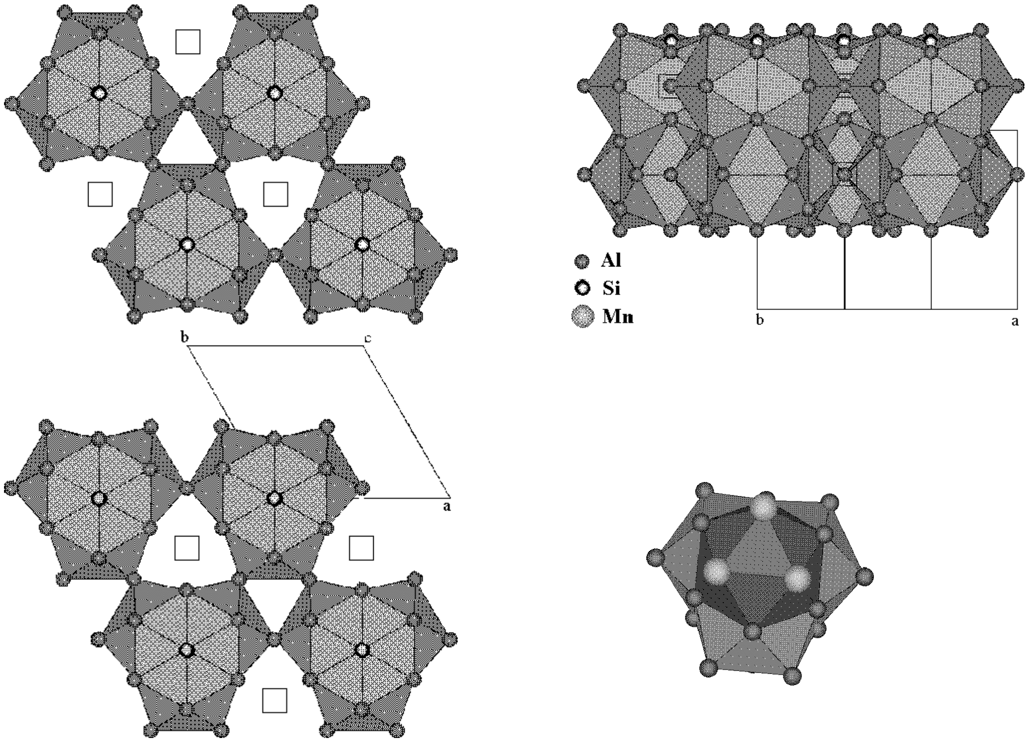

Figure 1. Crystal structure of $\beta\,\mathrm{Al_9Mn_3Si}$ phase described in terms of icosahedral clusters centered on the atoms. Si atoms are on Wyckoff site (2a). Squares show the sites of the vacancy Va (site (2d)). Top and side views of both layers at $z = \frac{1}{4}, \frac{3}{4}$ are shown. The icosahedral environment of each Si atom is also shown on the right low part of the figure.

First atom neighbours of the Mn site correspond to 10 Al/Si + 2 Mn atoms situated at vertices of a distorted icosahedron. Such an icosahedron is considered in the structural representation of $\beta\,\mathrm{Al_9Mn_3Si}$ (figure 1). The small Al(0)-TM, Al(1)-TM and Al(2)-TM distances suggest a strong effect of the sp-d hybridisation. Each Mn has two Mn first neighbours in Mn-triplet. Between Mn-triplets, Mn-Mn distances are about 4.17 Å. Similar Mn-triplets exist also in $\mu\,\mathrm{Al_{4.12}Mn}$ (hexagonal, P6$_3$/mmc, $\sim$563 atoms / unit cell) [3]. $\beta\,\mathrm{Al_9Mn_3Si}$ and $\varphi\,\mathrm{Al_{10}Mn_3}$ have significant relations with the complex structures $\mu\,\mathrm{Al_{4.12}Mn}$ and $\lambda\,\mathrm{Al_4Mn}$ (hexagonal, P6$_3$/m, $\sim$568 atoms / unit cell) [4] that are related to quasicrystals. For instance, in figure 1 of Ref. [3], the outline of the repeated unit of φ phase on several parts of μ structure is shown. Kreiner and Franzen [55, 4] showed that the I3-cluster, a structure unit of three vertex connected icosahedra, is the basic building block of a large number of intermetallic phases related to *i*-Al-Mn-Si such as $\alpha\,\mathrm{Al_9Mn_2Si}$, $\mu\,\mathrm{Al_{4.12}Mn}$ and $\lambda\,\mathrm{Al_4Mn}$. Note that the environment of Mn are also close to those found in α Al-Mn-Si approximant [10, 11, 12].

3.2. Vacancies

The hexagonal structure of Al_5Co_2 [5] is almost isomorphic with β and φ where Co replace Mn and Va sites (table 1). These phases have similar atomic sites and first-neighbours distances (table 2). However, a major difference is that the site (2d) is empty (Va) in β and φ whereas it is occupied by cobalt (Co(0)) in Al_5Co_2. It is thus interesting to understand why this vacancy is maintained in β and φ crystals? As first-neighbour distances around Mn in φ and β are similar to those around Co in Al_5Co_2, and that Va-Al distances in β and φ are very close of Co(0)-Al distances a vacancy can not be explained from steric encumbering. The environment of Va forms a Tri-capped trigonal prism (3 Al(1) and 6 Al(2)).

The same environment is also found in $\mu\,Al_{4.12}Mn$ [3] and $\lambda\,Al_4Mn$ [4]. But in μ and λ, this site is occupied by a Mn atom (Mn(1) in (2b) in $\mu\,Al_{4.12}Mn$ and Mn(1) in (2d) in $\lambda\,Al_4Mn$). In μ and λ, the first-neighbour distances Mn(1)-Al are $2.35-2.48\,\text{Å}$, which are similar to Va-Al first-neighbour distances in β and φ.

In the following, it is shown that the presence (or not) of such a vacancy in β and φ can be explained on account of the medium range atomic order because of strong Mn-Mn pair interaction up to medium range distances (more than $5\,\text{Å}$).

3.3. Role and position of Si atoms

The role of Si in Al based quasicrystals and related phases is known to have an important effect. Unstable quasicrystals are obtained in Al-Mn system, whereas stable quasicrystals are formed when a small proportion of Si is added [8]. Similar stabilising effects occurs for *i*-Al-Cu-Cr-Si [56] and for approximants α Al-Mn-Si [8], 1/1 Al-Cu-Fe-Si [57, 58], α Al-Re-Si [59]. The number of valence electrons are 3 (4) per Al (Si) atom. With respect to a Hume-Rothery condition for alloying ($2k_F \simeq K_p$), it is possible that a substitution of a small quantity of Si increases the e/a ratio in better agrement with $2k_F \simeq K_p$.

Experimentally Al and Si atoms have not been distinguished in $\beta\,Al_9Mn_3Si$. However, Robinson [1] has proposed to consider Si in (2a) because the interatomic distances between an atom on sites (2a) and its six neighbouring Al atoms is less than between any other pairs of Al atoms in β structure (table 2). But, from a comparison of β and φ, Taylor [2] has suggested that Si atoms should be preferentially in (12k) with Al atoms instead of (2a).

In section 4.2, we give arguments form *ab initio* calculations to understand the effect of Si on the Hume-Rothery stabilisation and to conclude that Si are likely in (2a).

4. First-principles calculations of the electronic structure

4.1. LMTO procedure, treatment of Si

Electronic structure determinations were performed in the frame-work of the local spin-density approximation (LSDA) [60] by using the *ab initio* Linear Muffin Tin Orbital method (LMTO) in an Atomic Sphere Approximation (ASA) [61, 62]. The space is divided into atomic spheres and interstitial region where the potential is spherically symmetric and flat, respectively. Sphere radii were chosen so that the total volume of spheres equals that of the solid. For vacancies (Va) empty spheres were introduced in (2d). The sphere radii are $R_{Si/Al(0)} = 1.37\,\text{Å}$, $R_{Al(1)} = R_{Al(2)} = 1.53\,\text{Å}$, $R_{Mn} = 1.34\,\text{Å}$, $R_{Va} = 1.04\,\text{Å}$ for β phase, and $R_{Al(0)} = 1.38\,\text{Å}$, $R_{Al(1)} = R_{Al(2)} = 1.55\,\text{Å}$, $R_{Mn} = 1.35\,\text{Å}$, $R_{Va} = 1.05\,\text{Å}$ for φ phase. As these structures are metallic and rather compacts, it was found that a small change of the sphere radii does not modify significantly the results.

Neglecting the spin-orbit coupling, a scalar relativistic LMTO-ASA code, was used with combined corrections for ASA [61, 62]. The **k** integration in a reduced Brillouin zone was performed according to the tetrahedron method [63] in order to calculate the electronic density of states (DOS). The final step of the self-consistent procedure and the DOS calculation were performed with 4416 **k** points in the reduced Brillouin zone. With an energy mesh equals to $\Delta E = 0.09\,\text{eV}$, calculated DOSs do not exhibit significant differences when the number of **k** points increases from 2160 to 4416. Thus, the structure in the DOS larger than 0.09 eV are not artefacts in calculations. Except in section 7, the LMTO DOSs calculations were performed without polarised spin (paramagnetic state).

The LMTO-ASA basis includes all angular moments up to $l = 2$ and the valence states are Al (3s, 3p, 3d), Mn (4s, 4p, 3d), Co (4s, 4p, 3d), Si (3s, 3p, 3d) and Va (1s, 2p, 3d) ‡. In order to analyse the position of Si atoms in the β phase, we performed calculations for $\beta(\text{Al},\text{Si})_{10}\text{Mn}_3$ where the Si atoms occupied randomly the Al sites. In this case an average atom named (Al,Si) was considered (virtual crystal approximation). In the LMTO-ASA procedure this atom is simulated with nuclear charge $Z = (1-c)Z_{Al} + cZ_{Si}$, where c is the proportion of Si atoms, and $Z_{Al} = 13$, $Z_{Si} = 14$ are the nuclear charge of Al, Si, respectively. Such a calculation can be justified as the main difference between Al and Si is the number of valence electrons. It was checked that the LMTO-ASA total energy of pure Al and pure Si are almost equal to this calculated with the average (Al,Si) atom with $c = 0.01$ and $c = 0.99$, respectively. Three possibilities were considered for the β phase: (i) the phase named $\beta\,\text{Al}_9\text{Mn}_3\text{Si}$ where Si are on site (2a) and Al, on site (6h) and site (12k); (ii) the phase $\beta\,\text{I-}(\text{Al},\text{Si})_{10}\text{Mn}_3$ where Si atoms substitute for some Al (on sites (2a), (6h) and (12k)); (iii) the phase $\beta\,\text{II-}(\text{Al},\text{Si})_{10}\text{Mn}_3$ where Si atoms substitute for some Al(2) (site (12k)). Same sphere radii for these three cases were input.

4.2. General aspects of the density of states (DOS)

Total energy self-consistent calculations were performed for different volumes, with isotropic volume changes i.e. the ratio c/a is constant and equal to the experimental value (table 1). The atomic positions were not relaxed. Minima of energy were obtained for a lattice parameter a equal to 7.41 Å for $\beta\,\text{Al}_9\text{Mn}_3\text{Si}$, 7.41 Å for $\beta\,\text{I-}(\text{Al},\text{Si})_{10}\text{Mn}_3$,

‡ In ASA approximation, orbitals are introduced in vacancies in order to yield a good expansion of the LMTO orbitals out of atomic spheres.

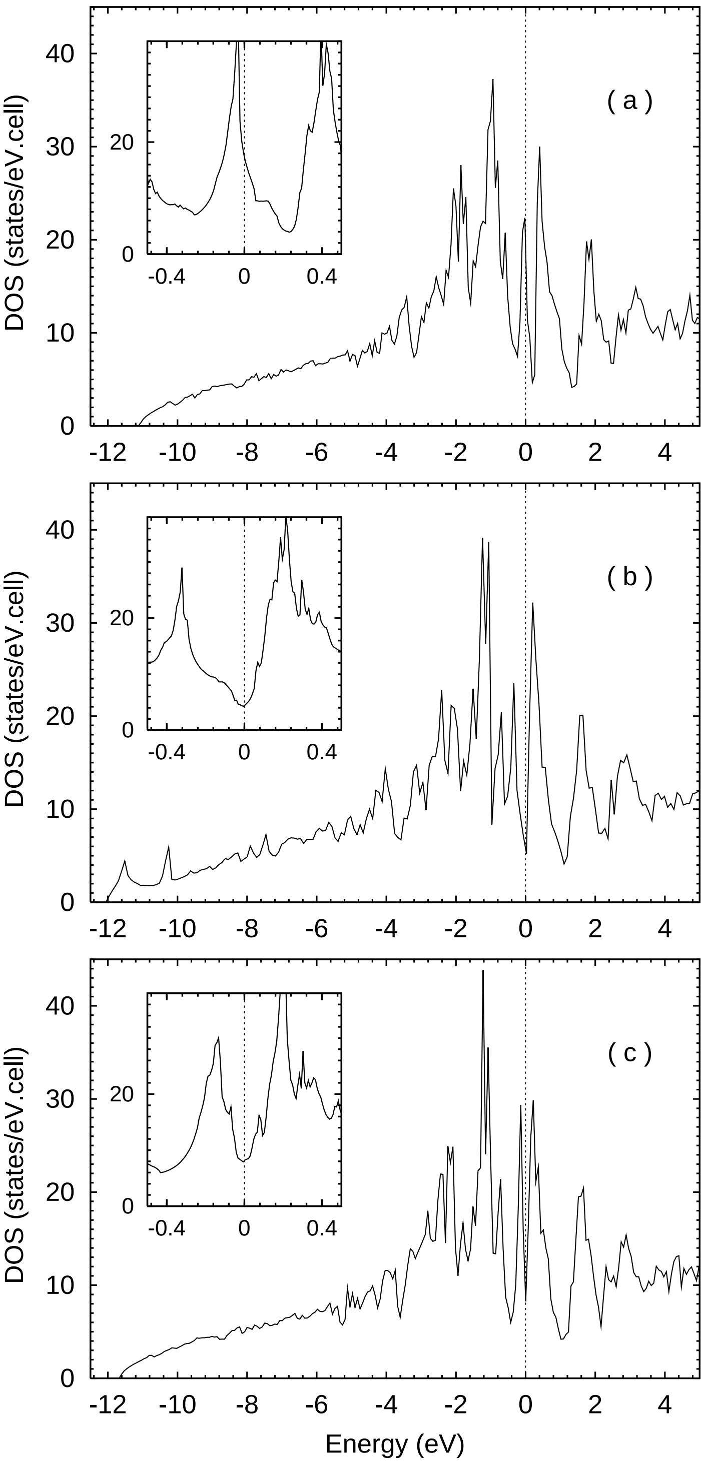

Figure 2. Total density of states (DOS) calculated by LMTO-ASA method in (a) $\varphi\,\mathrm{Al}_{10}\mathrm{Mn}_3$, (b) $\beta\,\mathrm{Al}_9\mathrm{Mn}_3\mathrm{Si}$, and (c) $\beta\,$I-$(\mathrm{Al},\mathrm{Si})_{10}\mathrm{Mn}_3$. Details of the total DOSs around E_F are given in inserts. $E_F = 0$. The DOS in $\beta\,$II-$(\mathrm{Al},\mathrm{Si})_{10}\mathrm{Mn}_3$ is almost the same as that in $\beta\,$I-$(\mathrm{Al},\mathrm{Si})_{10}\mathrm{Mn}_3$.

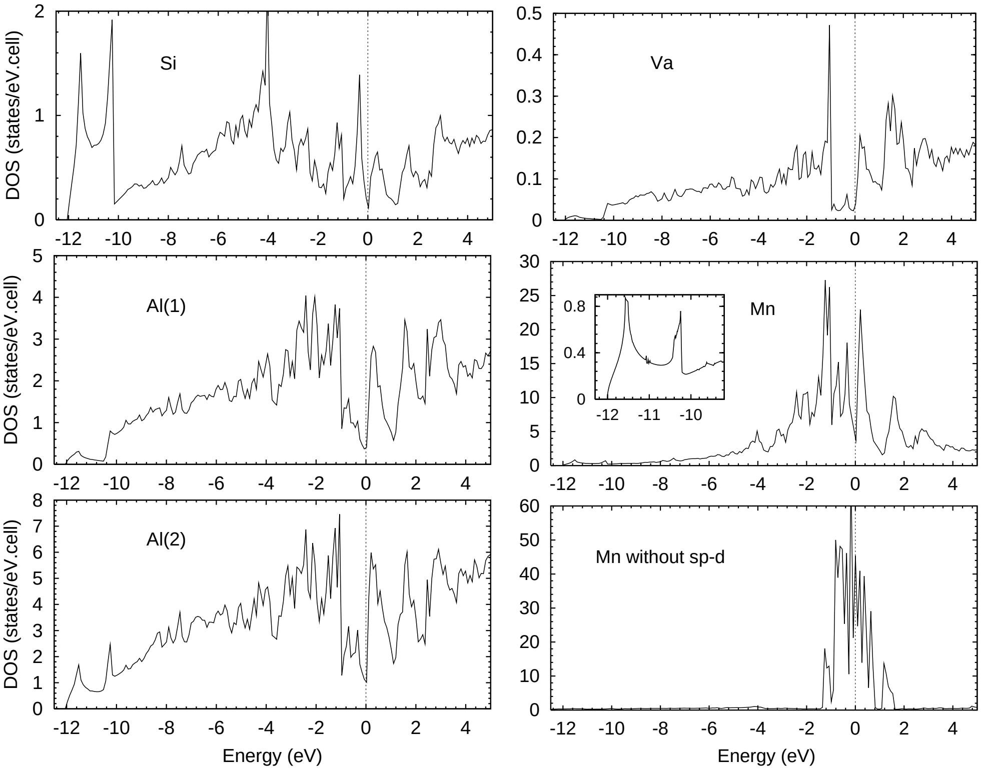

Figure 3. Local DOS performed by LMTO-ASA method in $\beta\,\mathrm{Al_9Mn_3Si}$ phase. Si are in (2a). The local Mn DOS calculated without sp-d hybridisation is also drawn (see text). $E_F = 0$.

7.42 Å for $\beta\,\mathrm{II\text{-}(Al,Si)_{10}Mn_3}$, and 7.43 Å for $\varphi\,\mathrm{Al_{10}Mn_3}$. These values correspond within 1.5 % to experimental values. Similar results have also been found in LMTO-ASA calculations for Al-TM alloys with small concentration of TM elements [14].

The total DOSs in β and φ phases (figure 2), are very similar. Local DOSs in β are also shown in figure 3. Except for low energies (less than -10 eV), the total DOS in β does not depend on the Si position. The parabola due to the Al nearly-free states is clearly seen. The large d band from -2 up to 2 eV is due to a strong sp-d hybridisation in agreement with experimental results [38, 39, 40, 64] and with first-principles calculations on Al-TM crystals and quasicrystals [14, 24, 47].

The sum of local DOSs on Al and Si atoms, shown in figure 4(a), is mainly sp DOS. As expected for a Hume-Rothery stabilisation, it exhibits a wide pseudogap near E_F due to electron scattering by Bragg planes of a predominant pseudo-Brillouin zone (i.e. the pseudo-Brillouin zone close to the Fermi surface). Its width of about 1 eV is of the same order of magnitude to this found in Al-Mn icosahedral approximants [14, 24, 45, 47]. The large pseudogap in $\{\mathrm{Al}+\mathrm{Si}\}$ DOS is meanly characteristic of a p-band at this energy, but the pseudogap in the total DOS is narrower. Therefore, the d states of Mn atoms must fill up partially the pseudogap. Nevertheless, as it is shown in the following that the pseudogap in $\{\mathrm{Al}+\mathrm{Si}\}$ DOS results from Mn sub-lattice effect.

Spiky total DOS where obtained for the studied phases as it has been found in

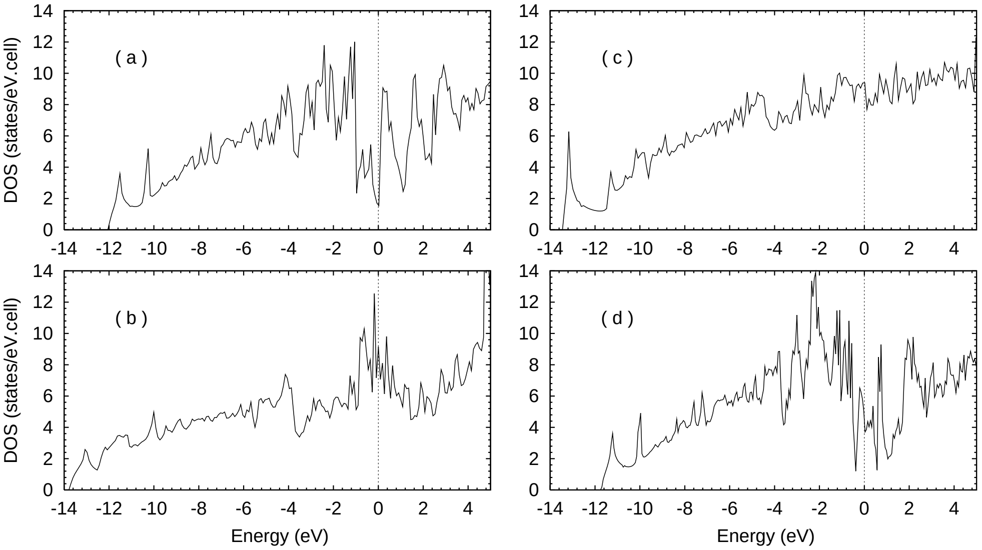

Figure 4. local {Al + Si} DOS performed by LMTO-ASA method in $\beta\,\mathrm{Al_9Mn_3Si}$ phase: (a) calculated including sp-d hybridisation, (b) calculated without sp-d hybridisation. (c) local {Al + Si} DOS in hypothetical $\beta\,\mathrm{Al_9Al_3Si}$ and (d) in hypothetical $\beta\,\mathrm{Al_9Mn_4Si}$. $E_F = 0$.

LMTO DOS of icosahedral small approximants (for instance α Al-Mn-Si [24], 1/1 Al-Cu-Fe [45], 1/1 Al-Pd-Mn [46]). In fact this is a consequence of a small electron velocity (flat dispersion relations) which contributes to anomalous electronic transport properties [24, 45, 65]. Such properties are not specific of quasicrystals as they are also observed in many crystal related to quasicrystals, therefore it does not only come from the long range quasiperiodicity. They are also associated with local and medium range atomic order that are related to quasiperiodicity. Indeed, it has been shown [66] that fine peaks in the DOS could come from electron confinement in atomic clusters characteristic [67] of the quasiperiodicity. This is not in contradiction with a Hume-Rothery mechanism because this tendency to localisation has a small effect on the band energy [66]. Whether spiky DOSs exist in quasicrystals or not is however much debated experimentally [49, 68, 43] and theoretically (Ref [69] and references therein) and the present calculation does not give answer to this question for the case of quasicrystals. But, in case of β and φ crystals, we checked that structures in the DOS with an energy scale larger than 0.09 eV are not artifacts in calculation as they do not depend on the non-physical parameters in the LMTO procedure (number of **k** points, see section 4.1).

4.3. Analysis of Si effect

From LMTO band energy calculated with fixed atomic positions and composition, the lowest band energy is obtain when Si atoms are in (2a) in $\beta\,\mathrm{Al_9Mn_3Si}$. The difference in band energy between $\beta\,\mathrm{Al_9Mn_3Si}$ and β I-$(\mathrm{Al,Si})_{10}\mathrm{Mn_3}$ is +5 eV / unit cell. The same order of magnitude is obtained between $\beta\,\mathrm{Al_9Mn_3Si}$ and β II-$(\mathrm{Al,Si})_{10}\mathrm{Mn_3}$. These *ab* *initio* results shows that Si are in (2a) and not mixed with Al. A comparison between the band energy of β and φ phases cannot be made because their compositions are different.

In the vicinity of E_F, the total DOSs in β and φ are very similar except E_F positions (figure 2). At E_F, the DOS is 5.6 states/eV.cell in β, 16.0 states/eV.cell in φ. The small amount of Si increases the average valence e/a in β. In a rigid band like model, this E_F shifts up to the minimum of the pseudogap, and in Hume-Rothery mechanism, the band energy is minimised. This difference allows one to understand why $\beta\,\mathrm{Al_9Mn_3Si}$ phase is stable whereas $\varphi\mathrm{Al_{10}Mn_3}$ phase is metastable.

Differences between $\beta\,(\mathrm{Al,Si})_{10}\mathrm{Mn_3}$ where Si atoms are mixed with Al atoms, and $\beta\,\mathrm{Al_9Mn_3Si}$ where Si atoms are in (2a) can also be understood from LMTO DOSs. Indeed, two bonding peaks are present at low energies (-11.5 eV and -10.3 eV, figure 3) in the local Si DOS of $\beta\,\mathrm{Al_9Mn_3Si}$, which is no more nearly-free states (each Si atom has 6 Al(2) and 6 Mn first neighbours (table 2)). The close proximity between Si and Mn and the presence of a bonding peak in the partial Mn DOS suggest that the Si-Mn bond is rather covalent and thus increases the stability of β phase when Si is on site (2a).

4.4. Effects of the d state of the transition-metal (TM) atoms

In this part the origin of the pseudogap is analysed from LMTO calculations for hypothetical phases derived from $\beta\,\mathrm{Al_9Mn_3Si}$. Three points are successively considered (*i*) the strong effect of the sp-d hybridisation on the pseudogap, (*ii*) the role of the Mn position which explains the origin of the vacancy (Va) in β and φ, (*iii*) and the great effect of Mn-Mn medium range interaction up to 5 Å.

(i) Role of the sp-d hybridisation on the pseudogap

Self-consistent LMTO calculation where performed without sp-d hybridisation by setting to zero the corresponding terms of the hamiltonian matrix [70]. Such a calculation is physically meaningful because the d TM states are mainly localised in the TM sphere and the sp Al states are delocalised. In figure 3, local Mn DOS (mainly d states), is drawn for two cases: with sp-d hybridisation and without sp-d hybridisation. The comparison between these local DOSs shows that the sp-d hybridisation increases the width of d band. This confirms a strong sp-d hybridisation. The local {Al + Si} DOS (mainly sp DOS) is also strongly affected by a sp-d hybridisation. As a matter of fact the pseudogap disappears in the calculation without sp-d hybridisation (figure 4(b)).

For Hume-Rothery alloys containing TM elements, a stabilisation mechanism is more complex than in sp alloys because of a strong sp-d hybridisation in the vicinity of E_F. Al and Si atoms, which have a weak potential, scatter sp electrons by a potential V_B almost energy independent. This leads to the so-called diffraction of electrons by Bragg planes in sp alloys. But the potential of Mn atoms depends on the energy. It is strong for energies around E_d, and creates a d resonance of the wave function that scatters also sp states. The effect is analysed in detail from a model hamiltonian in section 5. LMTO calculation was performed on hypothetical $\beta\,\mathrm{Al_9Al_3Si}$ constructed by putting Al in place of Mn in $\beta\,\mathrm{Al_9Mn_3Si}$ in order to confirm (or not) the previous analysis. The resulting total DOS (mainly sp DOS) of the hypothetical phase has no pronounced pseudogap (figure 4(c)). But there are many small depletions that might come from diffractions by Bragg planes. It shows that classical diffractions by Bragg planes by a weak potential V_B can not explain a pseudogap close to E_F in $\beta\,\mathrm{Al_9Al_3Si}$ and $\varphi\,\mathrm{Al_{10}Mn_3}$.

(ii) Effect of the Mn position, origin of the vacancy

As explained in section 3, a particularity of β and φ structures is a vacancy in (2d). This is the main difference with the $\mathrm{Al_5Co_2}$ structure (table 1). The origin of a vacancy can not be explained from too short near-neighbour distances (section 3.2). Therefore, a LMTO calculation was performed including a new Mn atom, named Mn(0), on site (2d) in $\beta\,\mathrm{Al_9Mn_3Si}$ phase using atomic sites and lattice parameters of $\beta\,\mathrm{Al_9Mn_3Si}$ (table 1). This hypothetical phase is named $\beta\,\mathrm{Al_9Mn_4Si}$ and its total and $\{\mathrm{Al+Si}\}$ DOSs are shown in figures 5 and 4(d), respectively. The absence of pseudogap in the total DOS results of a the great effect of Mn(0). In $\{\mathrm{Al+Si}\}$ DOS the pseudogap created by the scattering of sp electrons by the sub-lattice of Mn in (6h) is still present. But a large peak at E_F fills up partially the pseudogap. Consequently, E_F is located in a peak due to sp(Al)-d(Mn(0)) hybridisation. This is in fact a good example where a sp-d hybridisation does not induce a pseudogap. A similar result was obtained with an hypothetical $\varphi\,\mathrm{Al_{10}Mn_4}$, built by putting a Mn atom in place of the vacancy in (2d).

Total and local DOSs of hypothetical $\beta\,\mathrm{Al_9Mn_4Si}$ and $\mathrm{Al_5Co_2}$ [14, 38] are compared in figure 5. In spite of the near isomorphism between these structures, their DOSs are very different. As there is pseudogap in $\mathrm{Al_5Co_2}$ and not in $\beta\,\mathrm{Al_9Mn_4Si}$, it indicates that Co(0) and Mn(0) act differently, thus justifying the existence of a vacancy in both $\beta\,\mathrm{Al_9Mn_3Si}$ and $\varphi\,\mathrm{Al_{10}Mn_3}$ phases and not in $\mathrm{Al_5Co_2}$.

Therefore, the similar Wyckoff sites lead to both anti-bonding or bonding peaks depending on the nature of the atom on the Wyckoff site (2d), either Mn(0) or Co(0) respectively. Since there is a great effect of the nature of the TM element, a further analysis is proposed in section 6, where cohesive energies are compared using realistic TM-TM pair interaction.

(iii) Effect of Mn-Mn medium range interaction

The Mn-Mn distances in $\beta\,\mathrm{Al_9Mn_3Si}$ are reported in table 3. Mn are grouped together to form Mn-triplets (section 3.1). In order to determine the effect of a possible Mn-Mn medium range interaction on a pseudogap, a LMTO calculation was performed on a modified β phase containing only one Mn-triplet per unit cell instead of two. In this

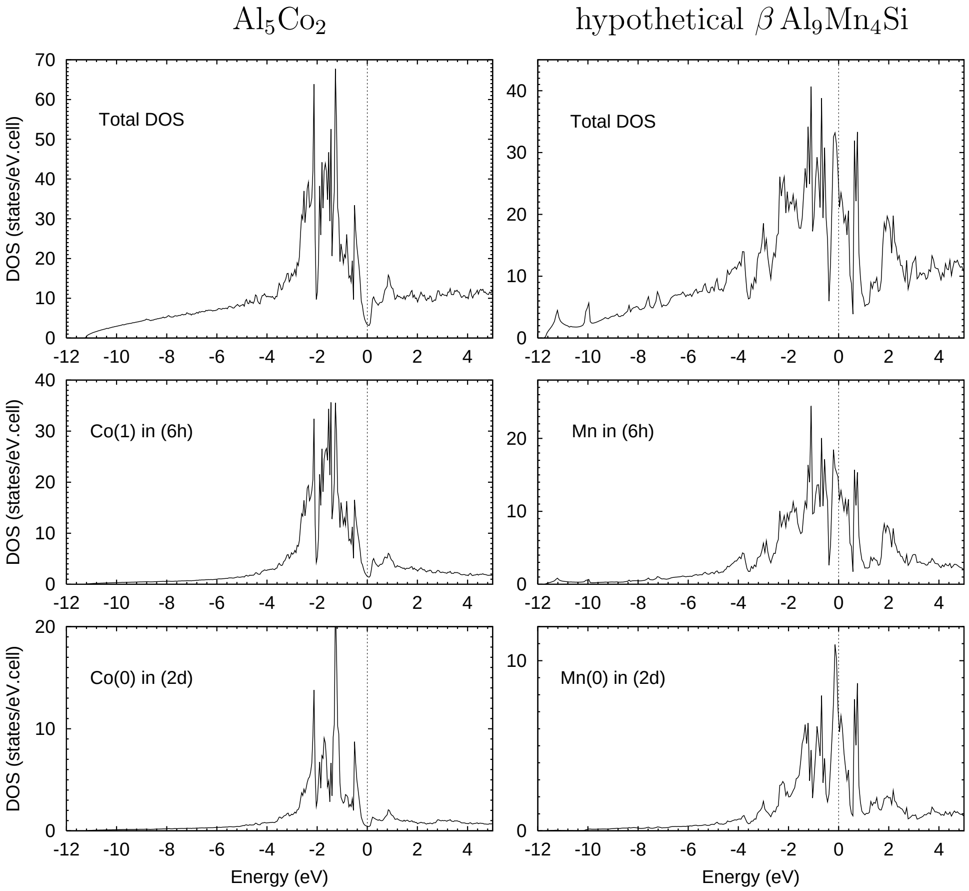

Figure 5. Total DOS and local TM DOSs performed by LMTO-ASA method in Al_5Co_2 and hypothetical $\beta\,Al_9Mn_4Si$. The $\beta\,Al_9Mn_4Si$ phase is built from $\beta\,Al_9Mn_3Si$ (table 1) by replacing the vacancy in (2d) by Mn atom (Mn(0)). Other Mn are in (6h). $E_F = 0$.

Table 3. Mn-Mn distances in $\beta\,Al_9Mn_3Si$ and hypothetical $\beta\,Al_9Mn_{1.5}Cu_{1.5}Si$ (see text).

Mn-Mn distance (Å)	Number of Mn-Mn pairs $\beta\,Al_9Mn_3Si$	$\beta\,Al_9Mn_{1.5}Cu_{1.5}Si$
2.69	2	2
4.17	4	
4.83	2	2
4.96	2	
6.38	4	
6.59	4	4
7.33	8	
7.51	6	6

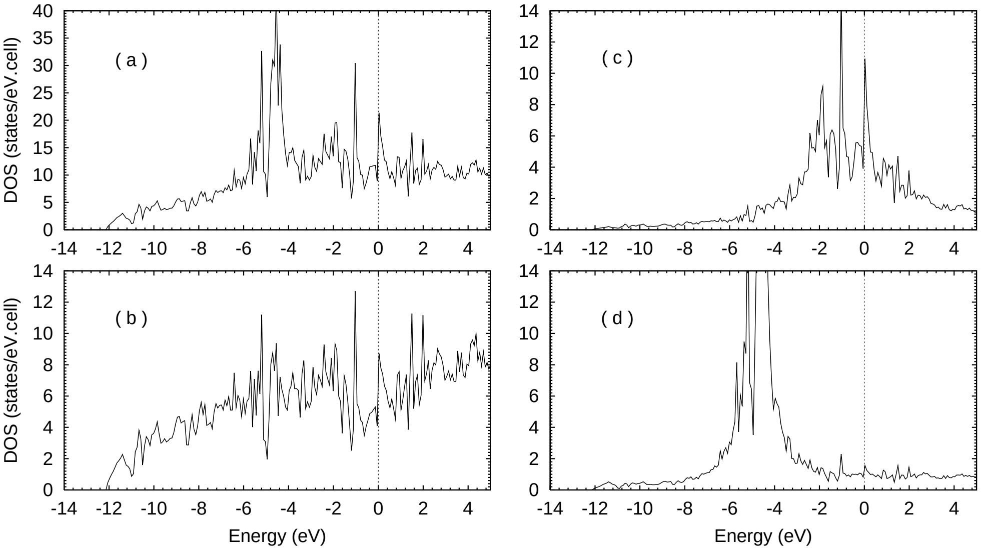

Figure 6. LMTO-ASA DOSs performed by LMTO-ASA method in hypothetical $\beta\,\mathrm{Al_9Mn_{1.5}Cu_{1.5}Si}$: (a) total DOS, (b) $\{\mathrm{Al}+\mathrm{Si}\}$ local DOS, (c) Mn local DOS, (d) Cu local DOS. The hypothetical $\beta\,\mathrm{Al_9Mn_{1.5}Cu_{1.5}Si}$ is built by placing 1 Mn-triplet by 1 Cu-triplet in each unit cell of $\beta\,\mathrm{Al_9Mn_3Si}$. $E_F = 0$.

case, $\beta\,\mathrm{Al_9Mn_3Si}$ was transformed into $\beta\,\mathrm{Al_9Mn_{1.5}Cu_{1.5}Si}$ by remplacing a Mn-triplet by a Cu-triplet. Mn environments remain identical up to 4.17 Å (table 3).

As results, the local Cu DOS (mainly d states, figure 6(d)) at E_F is very small; Cu having almost the same number of sp electrons as Mn, it has a minor effect near E_F. For the local Mn DOS the pseudogap disappears completely (figure 6(c)). For the total DOS, a small depletion below E_F is still remaining (figure 6(a)), and for the local $\{\mathrm{Al}+\mathrm{Si}\}$ DOS there is a pseudogap below E_F (figure 6(b)), but less pronounced than for $\beta\,\mathrm{Al_9Mn_3Si}$ (figure 4(a)). Therefore, such a disappearence of pseudogap proves the effect of Mn-Mn interactions over medium distances equal to 4.17, 4.96, 6.38 Å. . . (table 3).

5. Effective Bragg potential for sp states

5.1. Exitence of effective sp hamiltonian

As electrons are nearly-free electrons in Hume-Rothery sp crystals without TM atoms the hamiltonian writes [34],

$$H_{sp} = \frac{\hbar^2 k^2}{2m} + V_B. \tag{1}$$

V_B is a weak potential (Bragg potential), and does not depend on an energy,

$$V_B(\mathbf{r}) = \sum_{\mathbf{K}} V_B(\mathbf{K})\, \mathrm{e}^{i\mathbf{K}\cdot\mathbf{r}}, \tag{2}$$

where the vectors $\mathbf{K}$ belong to the reciprocal lattice. However, for alloys containing TM atoms, the strong scattering of sp electrons by TM atoms can not be described from a weak potential. In this case, a generalised Friedel-Anderson hamiltonian [71] has been considered. In a non-magnetic case:

$$H = H_{sp} + H_d + H_{sp\text{-}d} \ , \tag{3}$$

where sp states are delocalised nearly-free states (equation (1)) and d states are localised on d orbitals of TM atoms. H_d is the energy of d states. The term $H_{sp\text{-}d}$ represents a sp-d coupling which is essential in this context. The eigenstates ψ of H can be decomposed in two terms:

$$|\Psi\rangle = |\Psi_{sp}\rangle + |\Psi_d\rangle \ , \tag{4}$$

where Ψ_{sp} and Ψ_d are each linear combinations of sp states and linear combinations of d orbitals of all TM atoms. The classical tight-binding approximation $\langle\Psi_{sp}|\Psi_d\rangle = 0$ is made.

An *"effective Bragg potential"* for sp states, including effects of d orbitals of TM atoms, is calculated in order to analyse the effect of TM atoms. A projection of the Schrödinger equation, $(H - E)|\Psi\rangle = 0$, on the sub-space generated by sp states allows one to write the effective hamiltonian for sp states:

$$H_{eff(sp)} = \frac{\hbar^2 k^2}{2m} + V_{B,eff} \ \text{ with } \ V_{B,eff} = V_B + H_{sp\text{-}d} \frac{1}{E - H_d} H_{sp\text{-}d} \, , \tag{5}$$

and where V_B is as given by equation (2). The second term of $V_{B,eff}$ depends on energy. In crystals and quasicrystals, $V_{B,eff}$ is an effective Bragg potential that takes into account the scattering of sp states by the strong potential of TM atoms.

5.2. Characteristic of effective Bragg potential

For the phases presently considered, there are a few pairs of Mn atoms that are near-neighbours. Indeed each Mn is surrounded by 10 Al (Si) and 2 Mn (section 3). Therefore, a direct hoping between two d orbitals can be neglected. Thus:

$$H_d = \sum_{d,i} E_{di} \, |d,i\rangle\langle d,i| \ , \tag{6}$$

where i is a TM site index and d the five d orbitals of each TM atom. Assuming that all TM atoms are equivalent, one has $E_{di} = E_d$. The Fourier coefficients of the effective Bragg potential $V_{B,eff}$ are calculated from $H_{eff(sp)}$ using the formula $V_{B,eff}(\mathbf{K}) = \langle \mathbf{k}|H_{eff(sp)}|\mathbf{k} - \mathbf{K}\rangle$. One obtains:

$$V_{B,eff}(\mathbf{r}) = \sum_{\mathbf{K}} \left(V_B(\mathbf{K}) + \frac{|t_{\mathbf{k},\mathbf{K}}|^2}{E - E_d} \sum_i e^{-i\mathbf{K}.\mathbf{r}_i} \right) e^{i\mathbf{K}.\mathbf{r}} \ , \tag{7}$$

$$\text{where} \quad |t_{\mathbf{k},\mathbf{K}}|^2 = \sum_{d=1}^{5} \langle \mathbf{k}|H_{sp\text{-}d}|d_0\rangle\langle d_0|H_{sp\text{-}d}|\mathbf{k} - \mathbf{K}\rangle \ , \tag{8}$$

where $\mathbf{r}_i$ is the position of TM(i) atoms. By convention a TM atom with orbital d_0 is on a site at $\mathbf{r}_0 = 0$. $t_{\mathbf{k},\mathbf{K}}$ is a matrix element that couples sp states $|\mathbf{k}\rangle$ and $|\mathbf{k} - \mathbf{K}\rangle$ via sp-d hybridisation. The expression (7) is exact providing that a direct d-d coupling is neglected.

The potential of TM atoms is strong and creates d resonance of the wave function in an energy range $E_d - \Gamma \leq E \leq E_d + \Gamma$, where 2Γ is the width of the d resonance. In this energy range, the second term of equation (7) is essential as it does represent the diffraction of the sp electrons by a network of d orbitals, i.e. the factor $\left(\sum_i e^{-i\mathbf{K}.\mathbf{r}_{di}}\right)$ corresponding to the structure factor of the TM atoms sub-lattice. As the d band of Mn is almost half filled, $E_F \simeq E_d$, this factor is important for energy close to E_F. Note that the Bragg planes associated with the second term of equation (7) correspond to Bragg planes determined by diffraction. For β phase, it can be concluded that V_B has no effect on a pseudogap and on a phase stabilisation because of absences of pseudogap for DOS calculated for $\beta\,\mathrm{Al_9Mn_3Si}$ without sp-d hybridisation (figure 4(b)) and $\beta\,\mathrm{Al_9Al_3Si}$ without Mn atoms (figure 4(c)). Let us note however that the Hume-Rothery mechanism for alloying still minimizes the sp band energy due to a strong scattering of sp states by the Mn sub-lattice.

In summary, an analyse in term of effective Bragg potential allows one to interpret LMTO results as hybridisation-induced pseudogap in total and sp DOSs which comes from a diffraction of sp states by the sub-lattice of Mn atoms via the sp-d hybridisation. In this context the medium range distance between TM atoms might have important role.

6. Role of indirect Mn-Mn pair interaction

6.1. Medium range TM-TM interaction in Al based alloys

As a Hume-Rothery stabilisation is a consequence of oscillations of charge density of valence electrons with energy close to E_F [72, 34, 73, 74, 36], a most stable atomic structure is obtained when distances between atoms are multiples of the wavelength λ_F of electrons with energy close to E_F. Since the scattering of valence sp states by the Mn sub-lattice is strong, the Friedel oscillations of charge of sp electrons around Mn must have a strong effect on a stabilisation. Taking into account that stabilisation occurs for a specific Mn-Mn distance of 4.7 Å [75]. A Hume-Rothery mechanism in Al(rich)-TM compounds might be analysed in term of an indirect medium range TM-TM pair interaction resulting from a strong sp-d hybridisation. Zou and Carlsson [75, 76] have calculated this interaction from an Anderson model hamiltonian with two impurities, using a Green's function method. A calculation of an indirect TM-TM pair interaction, $\Phi_{TM\text{-}TM}$, within a multiple scattering approach [66] yields a result in good agreement with this given in Ref. [75] (figure 7). Mn-Mn [75, 76] and Co-Co [77, 78] interactions have been used successfully for molecular-dynamics studies [79, 80] of Al-Mn and Al-Co systems near the composition of quasicrystals.

As interaction magnitudes are larger for TM-TM than for Al-TM and Al-Al, $\Phi_{TM\text{-}TM}$ has a major effect on the electronic energy. Because of the sharp Fermi surface of Al, it asymptotic form at large TM-TM distance (r) is of the form:

$$\Phi_{TM\text{-}TM}(r) \propto \frac{\cos(2k_F\,r - \delta)}{r^3}\,. \tag{9}$$

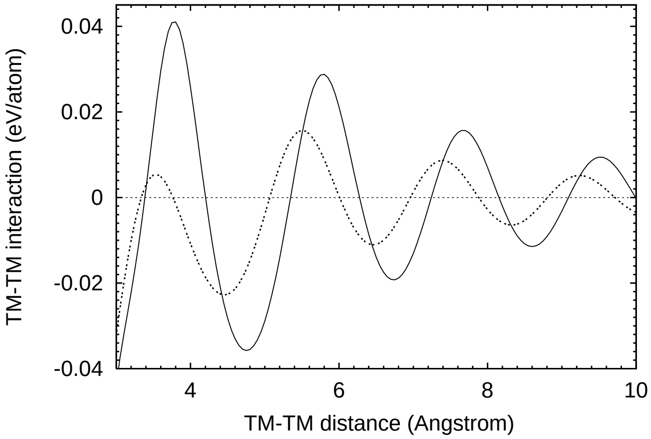

Figure 7. Indirect (solid lines) Mn-Mn pair interaction $\Phi_{Mn\text{-}Mn}$ and (dashed line) Co-Co pair interaction $\Phi_{Co\text{-}Co}$. This interaction does not include the short range repulsive term between two TM atoms. TM atoms are non-magnetic.

The phase shift δ depends on the nature of the TM atom and varies from 2π to 0 as the d band fills. Magnitude of the medium range interaction is larger for Mn-Mn than for other transition metal (Cr, Fe, Co, Ni, Cu), because the number of d electrons close to E_F is the largest for Mn, and the most delocalised electrons are electrons with Fermi energy. From the figure 7 and equation (9), it is clear that distances corresponding to minima of $\Phi_{TM\text{-}TM}$ depend also on the nature of TM atom.

6.2. Contribution of the medium range Mn-Mn interaction to total energy

The *"structural energy"*, $\mathcal{E}$, of TM sub-lattice in Al(Si) host is defined as the energy needed to built the TM sub-lattice in the metallic host that simulates Al and Si atoms from isolated TM atoms in the metallic host. $\mathcal{E}$ per unit cell is:

$$\mathcal{E} = \sum_{i,j\,(j\neq j)} \frac{1}{2}\,\Phi_{TM\text{-}TM}(r_{ij})\; e^{-\frac{r_{ij}}{L}}\ , \qquad (10)$$

where i and j are index of TM atom and r_{ij}, TM(i)-TM(j) distances. L is the mean-free path of electrons due to scattering by static disorder or phonons [81]. L depends on the structural quality and temperature and can only be estimated to be larger than 10 Å. Note that a similar exponential damping factor was introduced originaly in the treatment of RKKY interaction [82, 72]. In the following, the effects of TM-TM pairs over distances larger than first-neighbour distances is analysed. Therefore, an energy $\mathcal{E}'$ is calculated from equation (10) without including first-neighbour TM-TM terms in the sum. $\mathcal{E}'$ is the part of the structural energy of TM sub-lattice that only comes from medium range distances.

Structural energies, $\mathcal{E}'$, of the Mn sub-lattice are shown for $\beta\,Al_9Mn_3Si$ and $\varphi\,Al_{10}Mn_3$ structures in figure 8, where they are compared to those of $o\,Al_6Mn$ [83] and α Al-Mn-Si approximants [11, 12]. $\mathcal{E}'$ are always negative with magnitudes less

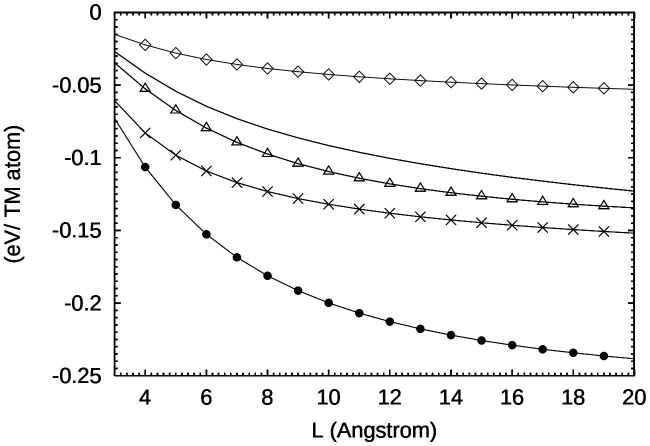

Figure 8. Structural energy $\mathcal{E}'$ of the Mn sub-lattice in (line) $\beta\,\mathrm{Al_9Mn_3Si}$, ($\triangle$) $\varphi\,\mathrm{Al_{10}Mn_3}$, ($\bullet$) o $\mathrm{Al_6Mn}$, ($\times$) α Al-Mn-Si, and ($\diamond$) hypothetical $\beta\,\mathrm{Al_9Mn_{1.5}Cu_{1.5}Si_{1.5}}$.

than $-0.1\,\mathrm{eV}\,/\,\mathrm{TM}$ atom, but strong enough to give a significant contribution to the band energy.

This result is in good agreement with an effect of Mn sub-lattice on the pseudogap as shown previously (sections 4.4 and 5). According to a Hume-Rothery mechanism, one expects that a pseudogap is well pronounced for a large value of $|\mathcal{E}'|$. Such a correlation is verified for the hypothetical $\beta\,\mathrm{Al_9Mn_{1.5}Cu_{1.5}Si}$ (section 4.4) where the diminution of pseudogap in $\beta\,\mathrm{Al_9Mn_{1.5}Cu_{1.5}Si}$ sp DOS (figure 6(b)) with respect to $\beta\,\mathrm{Al_9Mn_3Si}$ sp DOS (figure 4(a)), corresponds to reduction of ($|\mathcal{E}'|$) (figure 8).

6.3. Origin of the Vacancy

For structures containing serveral Mn Wyckoff sites, the TM-TM pair interaction mediated by conduction states allows one to compare the relative stability of TM atoms on different Wyckoff sites. Considering a phase with a structural energy of the TM sub-lattice equal to $\mathcal{E}$, the variation, $\Delta\mathcal{E}_i$, of $\mathcal{E}$ is determined when one TM(i) atom is removed from the structure:

$$\Delta\mathcal{E}_i = -\sum_{j\,(j\neq i)} \Phi_{TM\text{-}TM}(r_{ij})\; e^{-\frac{r_{ij}}{L}}\ . \tag{11}$$

TM atoms on different Wyckoff sites have different $\Delta\mathcal{E}_i$ values that can be compared. The most stable Mn sites correspond to highest $\Delta\mathcal{E}_i$ values. Moreover, the energy reference is a TM imputity in the Al(Si) matrix which does not depend on the structure. Therefore, it is possible to compare $\Delta\mathcal{E}_i$ calculated for different structures. As previously, the energy $\Delta\mathcal{E}'_i$ is calculated from equation (11) without the first-neighbour TM-TM contributions in order to analyse effects at medium range order.

Considering the hypothetical $\beta\,\mathrm{Al_9Mn_4Si}$ builted from $\beta\,\mathrm{Al_9Mn_3Si}$ in which a Mn atom (Mn(0)) replaces a vacancy (Va) in (2d), it appears that $\Delta\mathcal{E}'_{Mn(1)} > \Delta\mathcal{E}'_{Mn(0)}$ (figure 9). Mn(0) in (2d) is therefore less stable than Mn in (6h) for hypothetical $\beta\,\mathrm{Al_9Mn_4Si}$,

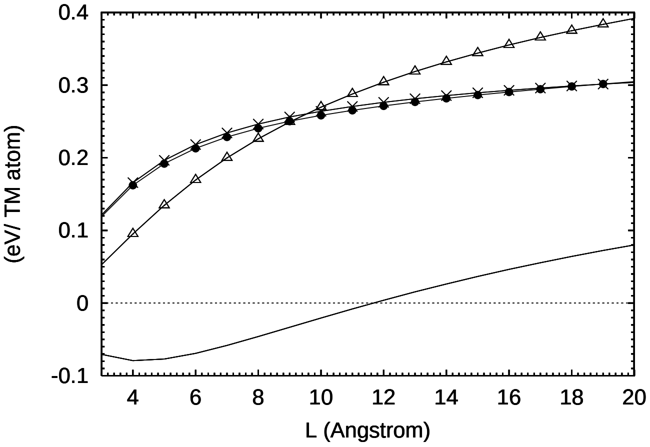

Figure 9. Variation of the structural energy $\Delta\mathcal{E}'_i$ due to Mn-Mn interaction for (simple line) Mn(0) in (2d) in the hypothetical $\beta\,Al_9Mn_4Si$; for (△) Mn in (6h) in the hypothetical $\beta\,Al_9Mn_4Si$; for (●) Mn(1) in (2b) in $\mu\,Al_{4.12}Mn$ [3]; and for (×) Mn(1) in (2d) in $\lambda\,Al_4Mn$ [4]. Mn(1) in $\mu\,Al_{4.12}Mn$ and $\lambda\,Al_4Mn$ have similar local environment as Mn(0) in hypothetical $\beta\,Al_9Mn_4Si$.

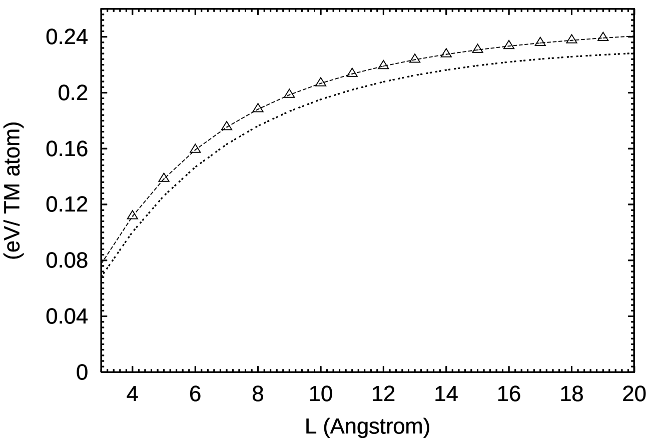

Figure 10. Variation of the structural energy $\Delta\mathcal{E}'_i$ due to Co-Co interaction in Al_5Co_2. $\Delta\mathcal{E}'_i$ is calculated for the two Co Wyckoff sites: (simple dashed line) Co(0) in (2d); (△) Co(1) in (6h).

thus justifying that a vacancy exists in β phase. A similar result was obtained for $\varphi\,Al_{10}Mn_3$.

On opposite, for complex crystals $\mu\,Al_{4.12}Mn$ [3] and $\lambda\,Al_4Mn$ [4] containing a Mn site (Mn(1) in Refs [3, 4]) with similar local environment as Va (or Mn(0)) in β structure (section 3.2), the corresponding $\Delta\mathcal{E}'_i$ values differs strongly from those of Mn(0) in hypothetical $\beta\,Al_9Mn_4Si$. Thus Mn(1) in μ and λ are more stable than an additional Mn atom replacing the vacancy in β and φ. Moreover, both $\Delta\mathcal{E}'_{Mn(1)}$ in μ and λ have the same order of magnitude as the $\Delta\mathcal{E}'_i$ calculated for other Mn(i) atoms in μ and λ (μ and λ phases contain 10 and 15 Mn Wyckoff sites respectively [3, 4]). Thus Mn(1) in μ and λ is stable. Such a difference between β, φ and μ, λ can be interpreted in terms of medium range Mn-Mn distances with respect to the curve of figure 7: In β, φ phases, environment of Va contains two Mn at distance 3.8 Å (table 2), whereas the smallest Mn(1)-Mn distance is 4.8 Å in μ and λ phases. 3.8 Å corresponds to an unstable Mn-Mn distance whereas 4.8 Å corresponds to a stable one (figure 7).

For Al_5Co_2 phase almost isomorphic of β and φ phases, there is a Co site (Co(0)) corresponding to the vacancy of β and φ (table 1). In this case $\Delta\mathcal{E}'_{Co(0)}$, calculated with a Co-Co pair interaction, is almost equal to $\Delta\mathcal{E}'_{Co(1)}$ (figure 10). As Co(0) in (2d) is as stable as Co(1) in (6h), it justifies why any vacancy does not exist in Al_5Co_2.

The present anaylsis on the origin of the vacancy in terms of TM-TM medium range interactions confirms the LMTO results (section 4.4). It shows the importance of TM-TM medium range indirect interaction on the atomic structure.

7. Magnetic properties

The presence of localised magnetic moments in quasicrystals and related phases containing Mn is much debated [13, 47, 85, 86, 87, 88, 89, 90, 91, 92, 93]. Vacancies, Mn pairs, triplets, quadruplets, quintuplets, variation of first-neighbour distances around Mn are often invoked to explain magnetic moments [94, 95, 96, 97, 98, 47, 92]. But in previous work [84, 99], it has been shown that an extreme sensitivity of magnetic properties also comes from an effect of an indirect Mn-Mn interaction mediated by sp states. Consequently an analysis limited to first-neighbour environments is not sufficient to interpret magnetic properties.

The unit cell of β and φ phases contains two Mn-triplets distant each other from from about 5 Å, and experimental measurements indicate that Mn-triplets are non-magnetic [89]. LMTO electronic structures calculated with polarised spin confirms that Mn triplets are non-magnetic in $\beta\,Al_9Mn_3Si$ and $\varphi\,Al_{10}Mn$. But from polarised spin LMTO calculation, performed on $\beta\,Al_9Mn_{1.5}Cu_{1.5}Si$ phase where a Cu-triplet replaces one Mn-triplet in each cell (section 4.4(*iii*) and table 3), a magnetic moment equal to $1\,\mu_B$ was found on each Mn in $\beta\,Al_9Mn_{1.5}Cu_{1.5}Si$ (i.e. 3 Mn in Mn-triplet are almost equivalent with a ferromagnetic spin orientation). The energy of formation of magnetic moments in $\beta\,Al_9Mn_{1.5}Cu_{1.5}Si$ is -0.046 eV per triplet. The Cu has no long range interaction as its d orbitals are full. Thus a medium range Mn-Mn interaction holds Mn-triplets in non-magnetic state whereas a Mn-triplet impurity in Al should be magnetic. It proves that a magnetic state of a Mn atom is very sensitive to surrounding Mn atoms at a medium range distance up to 4.17 Å (table 3). The model of the spin polarised Mn-Mn interaction presented in Ref. [84] is in agreement with this LMTO result.

As explain in the literature [13, 86, 47, 90, 99], the occurrence of magnetic Mn can be related to a reduction of pseudogap in the local Mn paramagnetic DOS in $\beta\,Al_9Mn_{1.5}Cu_{1.5}Si$ (figure 6(c)) by comparison with the local Mn DOS in $\beta\,Al_9Mn_3Si$ (figure 3). However, the present study shows that a pseudogap in paramagnetic Mn DOS does not only depend on the local environment of Mn as it is also very sensitive to Mn-Mn medium range interaction (sections 4.4(*iii*), 5.2 and 6.2).

8. Conclusion

From first-principles calculations combined with a model hamiltonian approach, it is shown that a detailed analysis of the electronic structure allows one to explain the following features of $\beta\,\mathrm{Al_9Mn_3Si}$ and $\varphi\,\mathrm{Al_{10}Mn_3}$ structures:

- The small amount of Si in $\beta\,\mathrm{Al_9Mn_3Si}$ stabilises its structure due to a shift of the Fermi energy toward the minimum of the pseudogap in the DOS. An *ab initio* study shows that, at 0 Kelvin, Si atoms are on a Wyckoff site different of those for Al atoms.
- $\beta\,\mathrm{Al_9Mn_3Si}$ and $\varphi\,\mathrm{Al_{10}Mn_3}$ are sp-d Hume-Rothery phases. The transition metal (TM) elements have a crucial effect as sp electrons are scattered by an effective Bragg potential dominated by the effect of the Mn sub-lattice. Such a Bragg potential relates to an indirect Mn-Mn interaction which has a strong magnitude up to $\sim 5\,\text{Å}$ and more.
- An analysis in terms of medium range TM-TM interactions gives theoretical arguments to understand the origin of a large vacancy existing in $\beta\,\mathrm{Al_9Mn_3Si}$ and $\varphi\,\mathrm{Al_{10}Mn_3}$, whereas similar sites are occupied by Mn in $\mu\,\mathrm{Al_{4.12}Mn}$ and $\lambda\,\mathrm{Al_4Mn}$, and by Co in $\mathrm{Al_5Co_2}$.

Finally, in $\beta\,\mathrm{Al_9Mn_3Si}$ and $\varphi\,\mathrm{Al_{10}Mn_3}$, the Hume-Rothery minimization of band energy leads to a “frustration” mechanism which favours a complex atomic structure. The Mn sub-lattice appears to be the skeleton of the stucture via a medium range indirect interactions between Mn atoms in the Al matrix. As β and φ structures are related to those of quasicrystals, it suggests that Hume-Rothery stabilisation, expressed in terms of Mn-Mn interactions, is intrinsically linked to the emergence of quasiperiodic structures in Al(Si)-Mn systems.

Acknowledgments

I am very grateful to D. Mayou with whom many ideas of this work have been developed. I thank also F. Hippert, D. Nguyen-Manh, R. Bellissent, V. Simonet and J. J. Préjean for fruitful discusions. My thanks to M. Audier from stimulating discussions and carefull reading of this paper.

References

[1] Robinson K 1952 *Acta Cryst.* **5** 397
[2] Taylor M A 1959 *Acta Cryst.* **12** 393
[3] Shoemaker C B, Keszler D A, Shoemaker D P 1989 *Acta Cryst.* **45** 13
[4] Kreinier G, Franzen H F 1997 *J. Alloys Comp.* **261** 83
[5] Newkirk J B, Black P J, Damjanovic A 1961 *Acta Cryst.* **14** 532
[6] Song S, Ryba E R 1992 *Phil. Mag. Lett.* **65** 85
[7] Shechtman D, Blech I, Gratias D, Cahn J W 1984 *Phys. Rev. Lett.* **53** 1951

[8] Berger C 1994 *Lecture on Quasicrystals* ed F Hippert and D Gratias (Les Ulis: Les Editions de Physique) p 463

[9] Hamerlin M, Maâmar S, Fries S, Lukas H L 1984 *Z. Metallkd.* **85** 814

[10] Cooper M, Robinson K 1966 *Acta Cryst.* **20** 614

[11] Guyot P, Audier M 1985 *Philos. Mag.* B **52** L15

[12] Elser V, Henley C L 1985 *Phys. Rev. Lett.* **55** 2883

[13] Trambly de Laissardière G, Nguyen Manh D, Mayou D 1993 *Europhys. Lett.* **21** 25

[14] Trambly de Laissardière G, Nguyen Manh D, Magaud L, Julien J P, Cyrot-Lackmann F, Mayou D 1995 *Phys. Rev.* B **52** 7920 (1995)

[15] Hume-Rothery W, Raynor G V 1954 *The Structure of Metals and Alloys* (London: Institute of Metals)

[16] Raynor G V, Waldron M B 1949 *Phil. Mag.* **40** 198

[17] Douglas A M B 1950 *Acta Cryst.* **3** 19

[18] Nicol A D I 1953 *Acta Crys.* **6** 285

[19] Raynor G V 1949 *Progr. Met. Phys.* **1** 1

[20] Hume-Rothery W, Coles B R 1954 *Adv. Phys.* **3** 149

[21] Friedel J, Dénoyer F 1987, *C. R. Acad. Sci. Paris Ser. II* **305** 171

[22] Friedel J 1988 *Helv. Phys. Acta* **61** 538

[23] Smith A P, Ashcroft N W 1987 *Phys. Rev. Lett.* **59** 1365

[24] Fujiwara T 1989 *Phys. Rev. B* **40** 942;
Fujiwara T, Yamamoto S, Trambly de Laissardière G 1993 *Phys. Rev. Lett.* **71** 4166

[25] Tsai A P, Inoue A, Masumoto T 1991 *Sci. Rep. Ritu.* A **36** 99

[26] Fujiwara T, Yokokawa T 1991 *Phys. Rev. Lett.* **66** 333

[27] Hafner J, Krajčí M 1992 *Europhys. Lett.* **17** 145

[28] Mayou D 1994 *Lecture on Quasicrystals* ed F Hippert and D Gratias (Les Ulis: Les Editions de Physique) p 417

[29] Gratias D, Calvayrac Y, Devaud-Rzepski J, Faudot F, Harmelin M, Quivy A, Bancel P A 1993 *J. Non Cryst. Solid* **153-154** 482

[30] Hippert F, Brand R A, Pelloth J, Calvayrac Y 1994 *J. Phys.: Condens. Matter* **6** 11189

[31] Sato H, Takeuchi T, Mizutani U 2001 *Phys. Rev.* B **64** 094207

[32] Mizutani U, Takeuchi T, Banno E, Fournée V, Takata M, Sato H 2001 *Quasicrystals* ed Belin-Ferré E, Thiel PA, Tsai AP and Urban K (Warrendale: Materials Research Society) *Mater. Res. Soc. Symp. Proc.* Vol. 643 p K13.1

[33] Tsai A P, Inoue A, Masumoto T 1989 *Mater. Trans. JIM* **30** 300; **30** 463

[34] Massalski T B, Mizutani U 1978 *Prog. Mater. Sci.* **22** 151

[35] Paxton A T, Methfessel M, Pettifor D G 1997 *Proc. R. Soc. Lond.* A **453** 1493

[36] Pettifor D G 2000 *The Science of Alloys for the 21st Century. A Hume-Rothery Symposium* ed P E A Turchi, R D Shull and A Gonis, TMS, 121

[37] Friedel J 1992 *Philos. Mag. B* **65** 1125

[38] Belin-Ferré, Trambly de Laissardière G, Pêcheur P, Sadoc A, Dubois J M 1997 *J. Phys.: Condens. Matter* **9** 9585

[39] Mori M, Matsuo S, Ishimasa T, Matsuura T, Kamiya K, Inokuchi H, Matsukawa T 1991 *J. Phys.: Condens. Matter* **3** 767

[40] Belin E, Kojnok J, Sadoc A, Traverse A, Harmelin M, Berger C, Dubois J M 1992 *J. Phys.: Condens. Matter* **4** 1057

[41] Belin E, Dankhazi Z, Sadoc A, Dubois J M, Calvayrac Y 1994 *Europhys. Lett.* **26** 677

[42] Belin E, Dankhazi Z, Sadoc A, Dubois J M 1994 *J. Phys.: Condens. Matter* **6** 8771

[43] Stadnik Z M, Purdie D, Baer Y, Lograsso T A 2001 *Phys. Rev. B* **64** 214202

[44] Fournée V, Belin-Ferré E, Pêcheur P, Tobala J, Dankházi Z, Sadoc A, Müller H 2002 *J Phys.: Condens. Matter* **14** 87

[45] Trambly de Laissardière G, Fujiwara T 1994 *Phys. Rev.* B **50** 5999

[46] Krajčí M, Windisch M, Hafner J, Kresse G, Mihalkovic M 1995 *Phys. Rev.* B **51** 17355

[47] Hafner J, Krajčí M 1998 *Phys. Rev.* B **57** 2849

[48] Stadnik Z M, Zhang G W, Tsai A P, Inoue A 1995 *Phys. Rev.* B **51** 11358; *Phys. Lett.* A **198** 237

[49] Stadnik Z M, Purdie D, Garnier M, Baer Y, Tsai A P, Inoue A, Edagawa K, Takeuchi S, Buschow K H J 1997 *Phys. Rev.* B **55** 10938

[50] Belin-Ferré E, Dankházi Z, Fournée V, Sadoc A, Berger C, Müller H, Kirchmayr H 1996 *J. Phys.: Condens. Matter* **8** 6213

[51] Trambly de Laissardière G, Fujiwara T 1994 *Phys. Rev.* B **50** 9843; *Mat. Sci. Eng.* A **181-182** 722

[52] Sabiryanov RF, Bose Sk, Burkov SE 1995 *J. Phys.: Condens. Matter* **7** 5437

[53] Krajčí M, Hafner J, Mihalkovič M 1997 *Phys. Rev.* B **62** 243

[54] Krajčí M, Hafner J, Mihalkovič M 1997 *Phys. Rev.* B **55** 843

[55] Kreiner G, Franzen H F 1995 *J. Alloys Comp.* **221** 15

[56] Khare V, Tiwari R S, Srivastava O N 2001 *Mat. Sci. Eng.* **304-306** 839

[57] Quivy A, Quiquandon M, Calvayrac, Faudot F, Gratias D, Berger C, Brand R A, Simonet V, Hippert F 1996 *J. Phys.: Condens. Matter* **8** 4223

[58] Takeuchi T, Yamada H, Takata M, Nakata T, Tanaka N, Mizutani U 2000 *Mat. Sci. Eng.* **294-296** 340

[59] Tamura R, Asao T, Takeuchi S 2001 *Phys. Rev. Lett.* **86** 3104

[60] von Barth U, Hedin L 1972 *J. Phys.* C **5** 1629

[61] Andersen O K 1975 *Phys. Rev. B* **12** 3060;
Andersen O K, Jepsen O, Gloötzel 1985 *Highlights of Condensed Matter Theory* ed F Bassani, F Fumi and M P Tosi (New York: North-Holland)

[62] Skriver H L 1984 *The LMTO Method* (New York: Springer)

[63] Jepsen O, Andersen O K 1971 *Solid State Commun.* **9** 1763

[64] Dankhazi Z, Trambly de Laissardière G, Nguyen-Manh D, Belin E, Mayou D 1993 *J. Phys.: Condens. Matter* **9** 3339

[65] Mayou D 2000 *Phys. Rev. Lett.* **85** 1290

[66] Trambly de Laissardière G, Mayou M 1997 *Phys. Rev.* B **55** 2890

[67] Gratias D, Puyraimond F, Quiquandon M, Katz A 2000 *Phys. Rev.* B **63** 24202

[68] Dolinšek J, Klanjšek M, Apih T, Smontara A, Lasjaunias J C, Dubois J M, Poon S J 2000 *Phys. Rev.* B **62** 8862

[69] Zijlstra E S, Janssen T 2000 *Europhys. Lett.* **52** 578

[70] Nguyen Manh D, Trambly de Laissardière G, Julien J P, Mayou D, Cyrot-Lackmann F 1992 *Solid State Commun.* **82** 329

[71] Anderson P W 1961 *Phys. Rev.* **124** 41

[72] Blandin A 1963 *Alloying Behaviour and Effects of Condentrated Solid Solutions* ed T B Massalski (New York: Gordon and Breach);
Blandin A 1967 *Phase Stability in Metals and Alloys* ed P S Rudman, J Stringer, R I Jaffee (New York: McGraw-Hill);
Blandin A 1980 *Physics-Bulletin* **31** 93

[73] Hafner J, von Heimendahl L 1979 *Phys. Rev. Lett.* **42** 386

[74] Hafner J 1987 *From Hamiltonians to Phase Diagrams* (Berlin: Springer Verlag)

[75] Zou J, Carlsson A E 1993 *Phys. Rev. Lett.* **70** 3748

[76] Zou J, Carlsson A E 1994 *Phys. Rev.* B **50** 99

[77] Phillips R, Zou J, Carlsson A E, Widom M 1994 *Phys. Rev.* B **49** 9322

[78] Moriarty J A, Widom M 1997 *Phys. Rev.* B **56** 7905

[79] Mihalkovič M, Zhu W J, Henley C L, Phillips R 1996 *phys. Rev.* B **53** 9021

[80] Mihalkovič M, Elhor H, Suck J B 2001 *Phys. Rev.* B **63** 214301

[81] Babić E, Krsnik R, Leontić B, Vučić Z, Zorić I, Rizzuto C 1971 *Phys. Rev. Lett.* **27** 805

[82] de Gennes P G 1962 *J. Phys. Radium* **23** 630

[83] Villars P, Calvert L D 1991 *Pearson's Handbook of Crystallographic Data for intermetallic Phases*

(American Society of Metals, Materials Park, OH) Vol 1

[84] Trambly de Laissardière G, Mayou D 2000 *Phys. Rev. Lett.* **85** 3273

[85] Berger C, Prejean J J 1990 *Phys. Rev. Lett.* **64** 1769;
Chernikov M A, Bernasconi A, Beeli C, Schilling A, Ott H R 1993 *Phys. Rev.* B**48** 3058;
Lasjaunias J C, Sulpice A, Keller N, Prejean J J 1995 *Phys. Rev.* B **52** 886

[86] Bratkovsky A M, Smirnov A V, Nguyen-Manh D, Pasturel A 1995 *Phys. Rev.* B **52** 3056

[87] Bahadur D 1997 *Prog. Crystal Growth and Charact.* **34** 287

[88] Hippert F, Audier M , Klein H, Bellissent R, Boursier D 1996, *Phys. Rev. Lett.* **76** 54

[89] Simonet V, Hippert F, Audier M, Trambly de Laissardière G 1998 *Phys. Rev.* B **58** 8865(R)

[90] Krajčí M, Hafner J 1998 *Phys. Rev.* **58** 14110

[91] Simonet V, Hippert F, Klein H, Audier M, Bellissent R, Fischer H, Murani A P, Boursier D 1998 *Phys Rev.* B **58** 6273

[92] Hippert F, Simonet V, Trambly de Laissardière G, Audier M, Y. Calvayrac Y 1999 *J. Phys.: Cond. Mat.* **11** 10419

[93] Préjean J J, Berger C, Sulpice A, Calvayrac Y 2002 *Phys. Rev.* B **65** 140203(R)

[94] Cooper J R, Miljak M 1976 *J. Phys. F* **6** 2151

[95] Hoshino T, Zeller R, Dederichs P H, Weinert M 1993 *Europhys. Lett.* **24** 495;
Hoshino T, Zeller R, Dederichs P H, Asada T 1996 *J. Magn. Magn. Mater* **156-158** 717

[96] Guenzburger D, Ellis D E 1991 *Phys. Rev. Lett.* **67** 3832

[97] Guenzburger D, Ellis D E 1994 *Phys. Rev.* B **49** 6004

[98] Scheffer M, Suck J B 2000 *Mat. Sci. Eng.* A **294-296** 629

[99] Trambly de Laissardière G, Mayou D 2000 *Mat. Sci. Eng.* A **294-296** 621